

# Frequency-doubling broadband light in multiple crystals

William J. Alford and Arlee V. Smith

*Department 1118, Lasers, Optics and Remote Sensing, Sandia National Laboratories, Albuquerque, New Mexico 87185-1423*

Manuscript received July 11, 2000; revised manuscript received November 27, 2000

We compare frequency doubling of broadband light in a single nonlinear crystal with doubling in five crystals with intercrystal temporal walk-off compensation and with doubling in five crystals adjusted for offset phase-matching frequencies. Using a plane-wave dispersive numerical model of frequency doubling, we study the bandwidth of the second harmonic and the conversion efficiency as functions of crystal length and fundamental irradiance. For low irradiance, the offset phase-matching arrangement has lower efficiency than a single crystal of the same total length but gives a broader second-harmonic bandwidth. The walk-off-compensated arrangement gives both higher conversion efficiency and broader bandwidth than a single crystal. At high irradiance, both multicrystal arrangements improve on the single-crystal efficiency while maintaining a broad bandwidth. © 2001 Optical Society of America

*OCIS codes:* 190.2620, 19.4410.

## 1. INTRODUCTION

Sometimes it is necessary to frequency mix broadband light in nonlinear crystals. If the broad bandwidth is associated with short, transform-limited pulses this mixing process is well understood. However, there are few systematic studies of nonlinear mixing of multiple-longitudinal-mode, or broadband, light. That is the subject of this paper. In single-crystal mixing the conversion efficiency suffers, and the bandwidth of the generated light narrows if the group-velocity walk-off between input and output waves exceeds the inverse of the input bandwidth—in other words, when the crystal acceptance bandwidth is less than the bandwidth of the input light. One suggested method for improving the mixing efficiency and also increasing the output bandwidth is to use multiple short crystals with their phase-matching wavelengths spread across the bandwidth of the input light. In this distributed  $\Delta k$  (DDK) arrangement, each crystal phase matches a different portion of the spectrum.<sup>1–4</sup> A second approach is to compensate for group-velocity walk-off between multiple short crystals.<sup>5,6</sup> This walk-off-compensated (WOC) arrangement effectively increases the acceptance bandwidth relative to a single crystal of the same total length by a factor equal to the number of crystals. A third approach is to disperse angularly the broadband fundamental light so that each spectral component propagates at its phase-matching angle in a critically phase-matched crystal.<sup>7</sup> In the context of femtosecond mixing this is often referred to as group-velocity-matched (GVM) mixing or tilted pulse-front mixing.<sup>8–10</sup> It relies on the combination of birefringent walk-off and tilted pulse fronts, perhaps in conjunction with noncollinear phase matching, to match the group velocities of the short pulses. This GVM mixing maximizes the effec-

tive acceptance bandwidth and efficiency in the plane-wave approximation.

All these doubling schemes can be evaluated analytically in the low-conversion, plane-wave limit. However, for strongly driven mixing a numerical model is essential. In this paper we use the numerical model of broadband mixing described in an earlier paper<sup>11</sup> (called method 1 in that paper). We are interested in the case in which the light's bandwidth is much greater than the transform of the pulse duration so that the temporal structure in the optical fields has a time scale much shorter than the pulse duration. We numerically construct such pulses by combining multiple longitudinal modes, giving them a Gaussian amplitude distribution and a random-phase distribution. This chaotic light stream is then multiplied by a Gaussian time profile to simulate a nanosecond-scale pulse from a multimode *Q*-switched laser. We numerically integrate a set of mixing equations that incorporate both group velocity and group-velocity dispersion but not diffraction or birefringent walk-off.<sup>11</sup> Diffraction and birefringent walk-off can be included<sup>12</sup> but at the expense of much longer computing times, and their inclusion is not expected to change the conclusions of the current research assuming that the beam diameters are large enough that the plane-wave approximation is valid. The numerical integration uses a split-step technique in which propagation is handled by fast Fourier methods whereas nonlinear interaction is handled by Runge–Kutta integration. As a concrete example we chose type I second-harmonic generation of a 420-nm, 1-ns (FWHM) pulse in a chain of five  $\beta$  barium borate (BBO) crystals or in a single crystal. The relevant properties of BBO are listed in Table 1. This choice of second-harmonic generation allows us to simplify our discus-

**Table 1. Properties of BBO for Doubling 420-nm Light**

Property	420 nm	Process	210 nm
Phase-matching angle		76°	
Nonlinear coefficient		0.5 pm/V	
Polarization	Ordinary		Extraordinary
Refractive index	1.689		1.689
Group velocity	$c/1.769$		$c/2.127$
Group-velocity dispersion	$-1.07 \times 10^5 \text{ cm/s cm}^{-1}$		$-3.16 \times 10^5 \text{ cm/s cm}^{-1}$
Temporal walk-off (420–210 nm)		1.2 ps/mm	
Acceptance bandwidth		14 $\text{cm}^{-1} \text{ mm}$	

sions, but many of our results can be extended to other three-wave mixing processes, and our numerical model is applicable to any such process. In the following sections we discuss first weakly driven, or low-conversion, mixing and then follow with a discussion of strongly driven mixing.

## 2. WEAKLY DRIVEN DOUBLING

Many of the properties of broadband frequency doubling can be derived analytically in the limit of low-conversion efficiency. For our example we use 1600 modes (Gaussian amplitude distribution and random-phase distribution) separated by 500 MHz so that the spectrum is filled uniformly from  $-400$  to  $+400$  GHz. We then multiply this spectrum by a Gaussian envelope with a width of 419 GHz ( $14 \text{ cm}^{-1}$ ) (FWHM). This chaotic light is strongly amplitude modulated and is a reasonable simulation of a broadband  $Q$ -switched laser. It is comprised of a train of spikes with more or less random phase and amplitude. The duration of the spikes is approximately the inverse of the bandwidth that, for our 419-GHz fundamental bandwidth, is approximately 2 ps. Temporal walk-off between the fundamental and the harmonic is 1.2 ps/mm because of their differing group velocities, so walk-off is important for crystals thicker than 100  $\mu\text{m}$ .

As a starting point for our discussion, we consider frequency doubling a single, 1-ps-long (FWHM), transform-limited pulse in a single 10-mm-long crystal. Our discussion is for plane waves only but we use irradiance levels corresponding to the center of a Gaussian profile of diameter 0.6 mm for added realism. Figure 1 shows results of a numerical simulation. The fundamental pulse is almost unchanged after passage through the crystal because the fundamental energy is small enough to keep mixing efficiency low. Because of its slower group velocity, the second-harmonic pulse is stretched in time to approximately 12 ps, the temporal walk-off between the fundamental and the harmonic. The leading edge of this stretched harmonic pulse is generated near the crystal's exit face, whereas the trailing edge is generated near the entrance face. In fact, each part of the fundamental field can be considered to generate a 12-ps-long square pulse of harmonic field, so the total harmonic field can be constructed when we add all these contributions. This summation yields the expression

$$\varepsilon_{\text{harm}}(t') = \kappa \int dt \varepsilon_{\text{fund}}^2(t' - t) S_{\tau}(t)/\tau, \quad (1)$$

where  $S_{\tau}(t)$  is a square-topped function with a width equal to the group-velocity walk-off  $\tau$ ,

$$S_{\tau}(t) = \begin{cases} 1 & \text{for } |t| < (\tau/2) \\ 0 & \text{for } |t| > (\tau/2), \end{cases} \quad (2)$$

and  $\kappa$  is a constant accounting for the nonlinear coefficient, the frequencies, and the refractive indices. Thus the harmonic field is a convolution of the square of the fundamental field and  $S_{\tau}(t)$ . The harmonic spectrum  $S_{\text{harm}}(\omega)$  is the Fourier transform of the harmonic field, and the transform of a convolution is the product of transforms for the two convolved functions, so

$$S_{\text{harm}}(\omega) = \mathcal{F}\{\varepsilon_{\text{fund}}^2(t)\} \mathcal{F}\{S_{\tau}(t)/\tau\}, \quad (3)$$

where  $\mathcal{F}\{\}$  represents a Fourier transform. The transform of the square function is a sinc function,

$$\mathcal{F}\{S_{\tau}(t)/\tau\} = \sqrt{\frac{1}{2\pi}} \text{sinc}(\Delta\omega\tau/2). \quad (4)$$

We refer to the sinc function as the envelope function throughout the remainder of the paper. For our 1-ps pulse,  $\mathcal{F}\{\varepsilon_{\text{fund}}^2(t)\}$  is a Gaussian of width (FWHM) 440 GHz, whereas

$$\mathcal{F}\{S_{12 \text{ ps}}(t)/12 \text{ ps}\} = \sqrt{\frac{1}{2\pi}} \text{sinc}(6 \text{ ps } \Delta\omega). \quad (5)$$

This sinc function has its first nulls at  $\nu = \pm 1/(12 \text{ ps}) = \pm 83 \text{ GHz}$ , so its width is twice the fundamental acceptance bandwidth of 42 GHz for a 10-mm-long BBO crystal (see Table 1). Figure 2 shows the power spectra for the fundamental and second harmonic, the latter being  $|S_{\text{harm}}(\omega)|^2$ .

As is well known, scanning a monochromatic laser across the phase-matched wavelength of a second-harmonic-generation crystal produces second harmonic with power proportional to  $\text{sinc}^2(\Delta k L/2)$ , where  $\Delta k = k_{2\omega} - 2k_{\omega}$ . Using the relationship between the group velocities,  $v_{\omega}$ , and  $k$ 's, we obtain

$$\frac{1}{v_{\omega}} = \frac{dk_{\omega}}{d\omega}, \quad (6)$$

and we can see that  $\Delta k$  is related to the detuning of the second harmonic from phase matching  $\Delta\omega$  by

$$\Delta k = \frac{dk_{2\omega}}{d\omega} \Delta\omega - \frac{dk_{\omega}}{d\omega} \Delta\omega = \left( \frac{1}{v_{2\omega}} - \frac{1}{v_{\omega}} \right) \Delta\omega, \quad (7)$$

so

$$\text{sinc}(\Delta kL/2) = \text{sinc}(\tau\Delta\omega/2). \quad (8)$$

Thus we can measure the envelope function by scanning a monochromatic laser across the phase-matching point.

We can find the second-harmonic fluence  $f_{\text{harm}}$  by integrating the spectral power over frequency

$$f_{\text{harm}} \propto \int d(\Delta\omega) |S(\Delta\omega)|^2. \quad (9)$$

According to Eq. (3), the fluence is proportional to the spectral integral of the product of the power spectrum of the fundamental field squared and the envelope function squared. If we could reduce the group-velocity walk-off  $\tau$ , the envelope function would broaden in  $\Delta\omega$  while maintaining its amplitude. According to relation (9), this would give a higher doubling efficiency. This reflects the fact that the quantity  $\int dt \varepsilon_{\text{harm}}(t)$  would be constant, in-

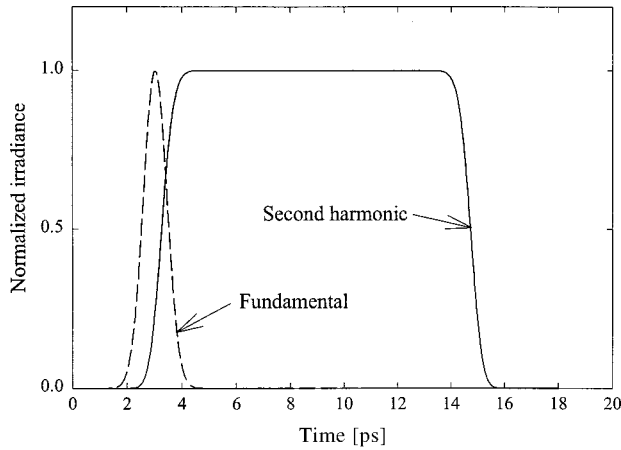


Fig. 1. Normalized irradiance of the fundamental and second-harmonic output from a 10-mm-long BBO crystal in the low-conversion regime. The input fundamental is a 1-ps (FWHM) Gaussian pulse. The second harmonic is stretched by 12 ps because of the group-velocity difference between the fundamental and the harmonic waves.

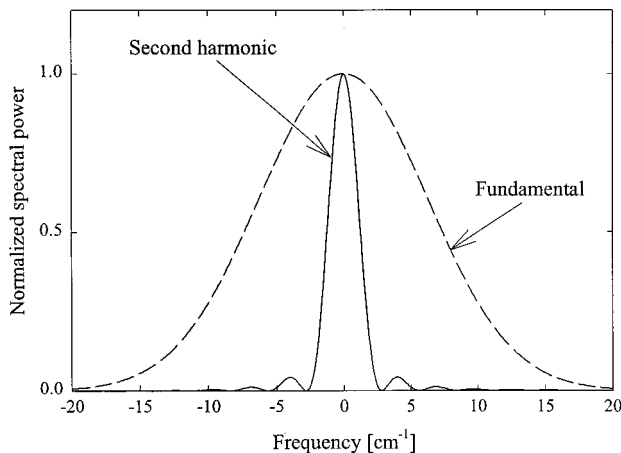


Fig. 2. Normalized spectra of the pulses of Fig. 1. The fundamental is a Gaussian of width (FWHM) 440 GHz ( $14.7 \text{ cm}^{-1}$ ). The harmonic is the product of a Gaussian and a  $|\text{sinc}(\Delta\omega t)|^2$  function with its first nulls at  $\pm 83 \text{ GHz}$  ( $2.8 \text{ cm}^{-1}$ ).

dependent of the walk-off time, but the quantity  $\int dt |\varepsilon_{\text{harm}}(t)|^2$  would increase, boosting the second-harmonic fluence.

Note that, although in the regime of low-conversion efficiency the second-harmonic spectrum is narrowed by temporal walk-off and the efficiency falls by approximately the ratio of the harmonic to the fundamental spectral width, this does not mean that only the spectral center of the fundamental wave is depleted, or that the conversion efficiency is limited by the crystal's acceptance bandwidth. The spectral wings contribute by sum-frequency mixing. Numerical simulation shows that the conversion efficiency can exceed 90% with little distortion of the fundamental spectrum. In addition, the harmonic spectrum changes relatively little, with the most noticeable change being that the secondary peak structure washes out. These claims can be verified by use of the function PW-mix-SP (plane wave-mix-short pulse) in the nonlinear optics software SNLO.<sup>10</sup>

### A. Single Crystal

From this understanding of short-pulse doubling we can predict the characteristics of broadband doubling in a single crystal. Each spike in the chaotic light generates a trailing, nearly square pulse of harmonic just as a solitary short pulse does. These overlap and interfere, but the resulting harmonic wave can once again be constructed as a convolution of the square of the fundamental field with the square-topped function of length equal to the walk-off. As before, the harmonic spectrum is  $|\mathcal{F}\{\varepsilon_{\text{fund}}^2(t)\}\mathcal{F}\{(S_\tau(t)/\tau)|^2|$ , but for broadband light  $\mathcal{F}\{\varepsilon_{\text{fund}}^2(t)\}$  is highly structured, reflecting the chaotic nature of the fundamental wave. The envelope of the spectrum is still  $[\text{sinc}^2(\Delta\omega\tau/2)/\sqrt{2\pi}]$ , implying that the width of the second-harmonic spectrum will be nearly the same as for the single, 1-ps pulse even though the harmonic pulse length is now approximately 700 ps rather than 12 ps. Figure 3 shows an example of such a spectrum, computed by our numerical model. In Fig. 3(a) we show the harmonic spectrum assuming that the fundamental and harmonic waves have identical group velocities (GVM). This is  $|\mathcal{F}\{\varepsilon_{\text{fund}}^2(t)\}|^2$ . Figure 3(b) is for a temporal walk-off of 12 ps. This is  $|\mathcal{F}\{\varepsilon_{\text{fund}}^2(t)\}|^2|\mathcal{F}\{S_{12}(t)/12 \text{ ps}\}|^2$ , so we expect the same spectral fine structure as in Fig. 3(a) but with different envelopes. In Fig. 4 we show an expanded view of these spectra near the zero-frequency offset point. Clearly the fine structure in the spectra are similar, as expected. The relative second-harmonic powers with and without walk-off are given by the ratio of their integrated spectral powers  $\int d(\Delta\omega) |S(\Delta\omega)|^2$ . With walk-off the power is reduced by approximately the ratio of the acceptance bandwidth to the fundamental spectral bandwidth.

An alternative method of estimating the relative powers is to compare both cases to doubling a 1-ns, single-longitudinal-mode pulse. The harmonic field at any time point is comprised of a sum of contributions from the fundamental over the preceding 12 ps. In the single-mode case these contributions add constructively because they all have the same phase, and they all have nearly the same amplitude because the fundamental amplitude variation over 12 ps is quite small. For our example, the

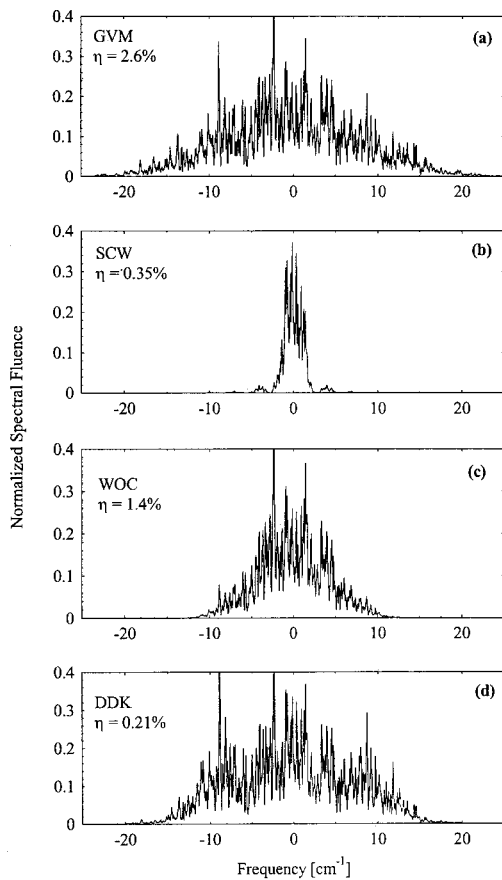


Fig. 3. Low-conversion efficiency normalized spectra of 210-nm second-harmonic (a) for a single crystal with matched fundamental and harmonic group velocities (GVM), (b) for a single crystal with actual BBO group-velocity difference (SCW) (c) for five WOC crystals; and (d) for five crystals with phase-matched frequencies at  $\Delta\omega = -13.9, -6.94, 0, 6.94, \text{ and } 13.9 \text{ cm}^{-1}$  (DDK). The fundamental input energy is  $10 \mu\text{J}$ , resulting in a fluence of  $2 \text{ mJ/cm}^2$ . The fundamental has a FWHM bandwidth of 419 GHz ( $14 \text{ cm}^{-1}$ ). The spectra are smoothed by use of a running average over  $0.14 \text{ cm}^{-1}$  to reduce the fine structure of the spectra for better readability. The spectrum of the input fundamental light is the same in each case. The  $\eta$ 's are doubling efficiencies.

doubling efficiency for the single-mode case is 1.3%. For the chaotic case with no walk-off we expect the efficiency to be twice as great, 2.6%, reflecting the well-known factor of 2 improvement for multimode light compared with single-mode light.<sup>13</sup> This is due to the spikey nature of chaotic light. Most of the energy is contained in amplitude spikes of a duration of approximately 2 ps for our bandwidth of 419 GHz. Our numerical model yields the expected 2.6% efficiency for zero walk-off. If we add walk-off there are approximately six uncorrelated contributions to the harmonic field at each time point, reflecting the 2-ps coherence time and the 12-ps walk-off time. This implies that the net harmonic field should be reduced by a factor of approximately  $\sqrt{6}$ . Squaring this to obtain an irradiance yields a reduction of roughly 6 relative to the zero walk-off case, or 3 relative to the single-mode case. The numerical model yields a slightly larger reduction of 3.7. The incoherent summation also means that the efficiency scales linearly with crystal length for chaotic light rather than quadratically as is characteristic of single-mode light. Another way of saying this is that

the chaotic efficiency is reduced by the ratio of the crystal acceptance bandwidth to the light bandwidth. However, just as in the case of doubling the 1-ps pulse, this does not mean that only the central portion of the fundamental spectrum is converted. The full fundamental spectrum contributes and is universally depleted.

### B. Multiple Crystals with Walk-Off Compensation

The effects of temporal walk-off can be reduced when we reverse the walk-off between mixing crystals. For wavelengths longer than those of our example, the birefringence of BBO can be used<sup>6</sup> to compensate walk-off, but we admit that for 420-nm doubling we know of no crystal with sufficient birefringence. Ignoring this practical difficulty, if we reconsider doubling a 1-ps pulse, walk-off compensation would reduce the width of the second-harmonic pulse from 12 ps to approximately 3 ps, the convolution of the 1-ps pulse and a 2.4-ps ( $=12 \text{ ps}/5$ ) square pulse. The harmonic field would be correspondingly stronger by a factor of 4 or so. Irradiance would be 16 times higher but duration would be 4 times smaller, implying a conversion efficiency 4 times higher than for the single 10-mm crystal. The shorter duration also translates to a broader harmonic spectrum. More quantitatively, the square-topped convolution function has a width of 2.4 ps, so the envelope function is

$$\mathcal{F}\{S_{2.4 \text{ ps}}(t)/2.4 \text{ ps}\} = \sqrt{\frac{1}{2\pi}} \text{sinc}(1.2 \text{ ps } \Delta\omega). \quad (10)$$

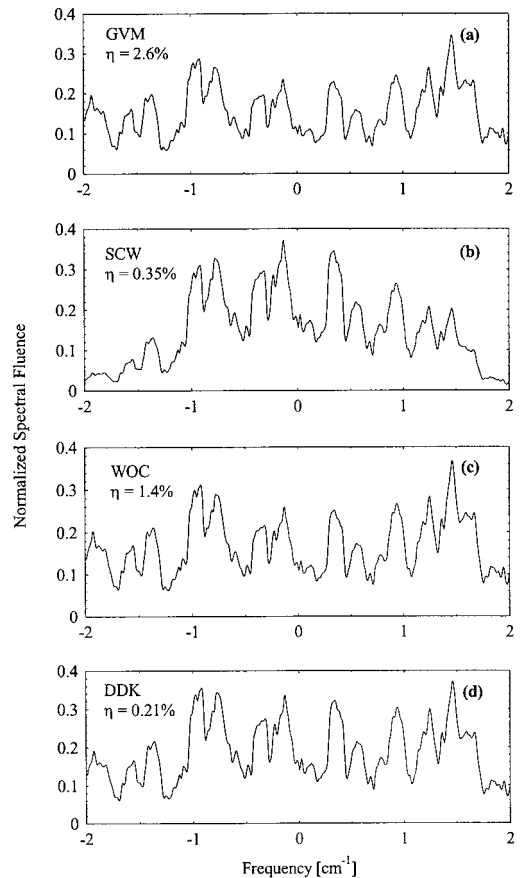


Fig. 4. Expanded view of the spectra of Fig. 3 showing that the harmonic spectra are similar in each case.

Its peak height is unchanged but its width is five times that of the uncompensated case with the same total crystal length.

For a chaotic fundamental field, the harmonic field is again the convolution of the square of the fundamental field with the 2.4-ps-wide square pulse. The first nulls of the sinc envelope should lie at  $\pm 420$  GHz. This is illustrated in the model-generated spectrum shown in Fig. 3(c). Figure 4(c) shows that the structure at the center of the spectrum is again  $|\mathcal{F}\{\epsilon_{\text{fund}}^2(t)\}|^2$ , unchanged by walk-off compensation.

Walk-off compensation means that each time point in the second-harmonic pulse receives contributions from the preceding 2.4 ps of fundamental rather than the preceding 12 ps. The number of uncorrelated contributions is thus approximately 1.2 rather than 6. Furthermore, each point receives equal contributions from each of the five crystals. Taken together these effects should increase the efficiency relative to the uncompensated chaotic case by a factor of nearly 5. The actual enhancement in our example is 4.0. The higher efficiency is associated with a factor of 5 broadening of the envelope function.

### C. Multiple Crystals with Offset $\Delta k$ 's

An alternative method of broadening the spectrum of doubled chaotic light is to use multiple crystals with each adjusted to phase match a different portion of the fundamental spectrum (DDK). Admittedly this is a misleading description of the doubling process because, as we stated above, frequency doubling depletes the entire fundamental spectrum even though the harmonic spectrum is narrowed to the crystal's acceptance bandwidth. Returning to the 1-ps pulse, if a crystal has a nonzero phase-velocity mismatch ( $\Delta k \neq 0$ ), the contributions to the harmonic pulse from different positions in the crystal have different phases, so the square pulse  $S_r(t)$  is replaced by  $S_r(t)\exp(i\Delta k L t/\tau)$ . The Fourier transform of this is a sinc function centered at  $\omega_0 = -(\Delta k L)/\tau$ . So the spectrum is  $|G_{440}(\Delta\omega)|^2 |\text{sinc}(\tau\Delta\omega + \Delta k L/\tau)|^2$  where  $G_{440}(\Delta\omega)$  is a Gaussian of width 440 GHz, the transform of the 1-ps Gaussian fundamental pulse. If the single 10-mm crystal in our example is replaced by five crystals, each 2 mm long, and each with a different phase mismatch  $\Delta k$ , the function  $S_r \exp(i\Delta k L t/\tau)$  is replaced by a sequence of five square pulses, each 2.4 ps long, and each with a phase chirp, or frequency offset of  $\omega_0 = -(\Delta k 2 \text{ mm})/(2.4 \text{ ps})$  appropriate to its individual value of  $\Delta k$ . The phases of these square pulses splice together without phase discontinuities. The envelope function is then the Fourier transform of this 12-ps-long square-topped pulse that has five zones with different phase chirps. A reasonable spacing of the phase-matching centers is half of the acceptance bandwidth for a 2-mm crystal, or  $6.9 \text{ cm}^{-1}$ . This set of  $\Delta k$ 's can be sequenced in 30 distinct orders, but only those with offsets sequenced red to blue or vice versa produce an envelope function without deep interference dips near the line center. This envelope function is shown in Fig. 5. It is approximately five times wider than for the single crystal but is also approximately ten times lower in maximum value. We verified that our numerical model also gives this envelope function by dividing the model-generated DDK harmonic spectrum by the corresponding

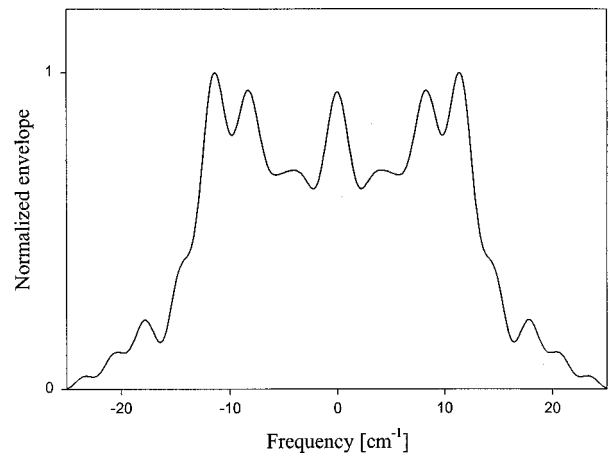


Fig. 5. Envelope function for five crystals with detunings  $\Delta\omega = -13.9, -6.94, 0, 6.94, \text{ and } 13.9 \text{ cm}^{-1}$ .

GVM spectrum. Envelope functions for other crystal sequences have the same area but tend to be more spread in frequency with deep interference dips. The product of the envelope function with  $|\mathcal{F}\{\epsilon_{\text{fund}}^2(t)\}|^2$  is shown in Fig. 3(d) and is expanded in Fig. 4(d). The doubling efficiency for our example is 0.21%, less than for the GVM case (2.6%), the single crystal with walk-off (SCW) (0.35%), or the WOC crystals (1.4%).

As we showed above, tuning monochromatic fundamental light across the phase-matched zone also maps out the envelope function. That is the analysis approach of Brown<sup>1</sup> and of Babushkin *et al.*<sup>2</sup> Brown used a plane-wave, monochromatic model to compute the conversion versus the frequency in six crystals with detunings approximately equal to an acceptance bandwidth. She also tested this experimentally by doubling 250-ns pulses of broadband 972-nm light in six type I BBO crystals, each 2.5 mm in length. The second harmonic was then doubled to 243 nm in another set of six type I BBO crystals. She verified the expanded spectrum of the 243-nm light relative to that expected for a single crystal of the same length. However, she did not compare the efficiency of these two methods. Babushkin *et al.* did similar experiments using two type II KDP crystals to sum single-mode, 100-ps pulses of 532- and 1064-nm light. Their crystal lengths were 9 and 16 mm. They used beam tilt to simulate frequency tuning and mapped envelope functions for fixed crystal angles but with varying intercrystal phase shifts.

### D. Summary of Weakly Driven Doubling

In weakly driven second-harmonic generation the fundamental wave is altered little by frequency doubling. We showed that in this case the second-harmonic spectra are given by the product of the Fourier transform of the square of the fundamental field  $\mathcal{F}\{\epsilon_{\text{fund}}^2(t)\}$  and an envelope function that characterizes group-velocity walk-off and phase mismatch in the crystal or set of crystals. The former is the same for all arrangements, meaning that the envelope functions determine the efficiencies because conversion efficiency is proportional to the integrated spectral power. This makes it quite easy to calculate the doubling efficiency for broadband light relative to that for

an otherwise identical monochromatic pulse. The envelope function can be calculated by the group-velocity walk-off and phase-velocity mismatches for the crystals, or it can be measured by scanning a monochromatic laser across the phase-matching region.

Using a numerical model, we showed that the doubling efficiency for chaotic light is twice that of monochromatic light if the acceptance bandwidth of the crystal is much larger than the bandwidth of the chaotic light. When the bandwidth of the light is broad compared with the acceptance bandwidth, both the numerical model and our analytical calculations show that mixing in  $N$  crystals of length  $L/N$  with walk-off compensation between them is equivalent to reducing the walk-off by a factor of  $N$ , causing an increase in the acceptance bandwidth by  $N$ . The doubling efficiency is improved by a comparable amount. Alternatively, the bandwidth of the second-harmonic light can be increased by use of several short crystals tilted so that their phase-matching wavelengths are distributed over the bandwidth of the broadband fundamental. The resulting efficiency is much less than for walk-off compensation and is less than for a single crystal. The shape of the envelope function for this arrangement is sensitive to the order of the phase mismatches with the preferred sequence being monotonic red to blue or blue to red.

The analysis methods described here are applicable to other mixing processes as long as the input waves have matched group velocities and the conversion is low. The input group velocities can often be matched by use of non-collinear phase matching.<sup>10</sup> Our analysis method is also applicable to mixing broadband light with single-longitudinal-mode light, whether the input group velocities are matched or not, as long as the pulse lengths are much greater than the temporal walk-off.

### 3. STRONGLY DRIVEN DOUBLING

Our analysis of weakly driven doubling breaks down in the strongly driven case because it was based on the assumption that the fundamental wave is unaltered by doubling. In strong mixing the temporal and spectral structure of the fundamental can be altered drastically, in which case broadband doubling can be analyzed accurately only by use of numerical models with group-velocity effects included, such as those of Milonni *et al.*<sup>4</sup> or Smith and Gehr.<sup>11</sup> In this section we present model results for the same cases discussed above except the fundamental energy and the crystal lengths were increased to reach the high-conversion regime. We use the same chaotic fundamental light as before but scale up its energy. The damage fluence of BBO sets the upper limit on pulse energy.

Figure 6 shows second-harmonic spectra for the same cases as before but with the fundamental input energy increased from  $10 \mu\text{J}$  to  $10 \text{mJ}$ . The conversion efficiency for a single-mode pulse is 98% under these conditions. For chaotic light but with no walk-off, Fig. 6(a), the efficiency is 95%. The expanded spectrum, shown in Fig. 7(a), is different from the low-conversion case [compare with Fig. 4(a)], but not by a large amount. When walk-off is included, the efficiency is reduced to 22%, and the spectrum is changed dramatically [Fig. 7(b)].

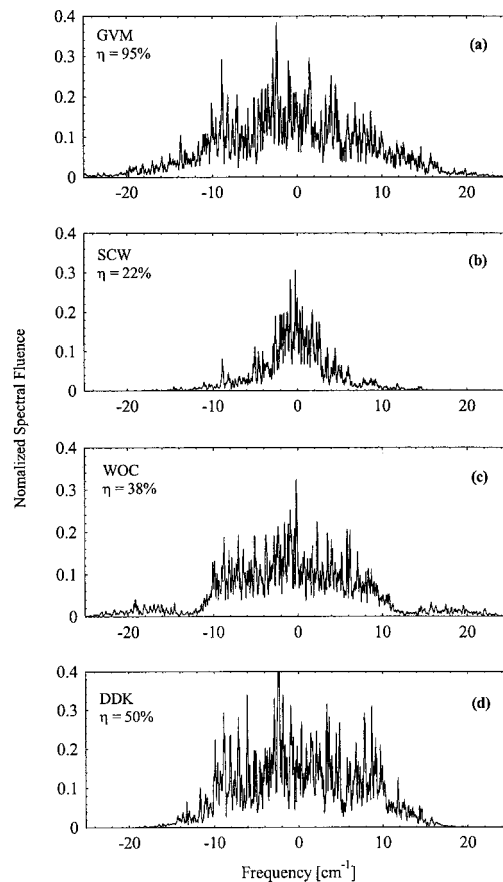


Fig. 6. High-conversion efficiency normalized harmonic spectra under the same conditions as Fig. 3 except the fundamental pulse energy is increased from  $10 \mu\text{J}$  to  $10 \text{mJ}$ .

In Fig. 8 we plot a conversion efficiency surface for a single crystal without walk-off (GVM). As expected, the efficiency approaches 100% with sufficient pulse energy and crystal length. Interestingly, Fig. 8 shows that even this case can be overdriven. At high values of crystal length and pulse energy, the efficiency drops below its maximum. This is due to group-velocity dispersion that changes the relative local phases of the fundamental and harmonic, allowing some backconversion from the harmonic to the fundamental. If the group-velocity dispersions are set to zero, the hanging valley on the efficiency surface is raised to nearly 100%.

Figure 9 is the same as Fig. 8 except we include walk-off (SCW). The maximum conversion efficiency falls from almost 100% to approximately 30%. The shape of the harmonic spectral envelope shown in Fig. 6(b) is quite different from the weak doubling case. The sidelobes have risen and the modulation has washed out. This is to be contrasted with the profile that we traced out by scanning a monochromatic laser across the phase-matching region. At high doubling efficiency such a scan produces a spectral shape with distinct sidelobes but with a narrowed rather than broadened main peak,<sup>14–16</sup> so scanning a single-mode laser is not a useful measure of the harmonic envelope for strongly driven second-harmonic generation.

Figure 10 shows the efficiency surface for five WOC crystals. There is a small zone where the efficiency is quite high, but as in the case of the single crystal it is pos-

sible to overdrive the crystals so that the efficiency falls with increasing energy or crystal length. When this occurs the harmonic spectrum is also strongly modified, as shown in Fig. 7(c). In Fig. 6(c) we can see that the envelope function is now nearly square topped with sidelobes.

Figure 11 shows the efficiency surface for five crystals with distributed  $\Delta k$ 's (DDK). This arrangement does not suffer from decreasing efficiency with increasing input energy within the range of the figure. The spectral envelope function [Fig. 6(d)] looks much like that at low efficiency [Fig. 3(d)] even though the spectral fine structure is highly altered [compare with Figs. 4(d) and 7(d)].

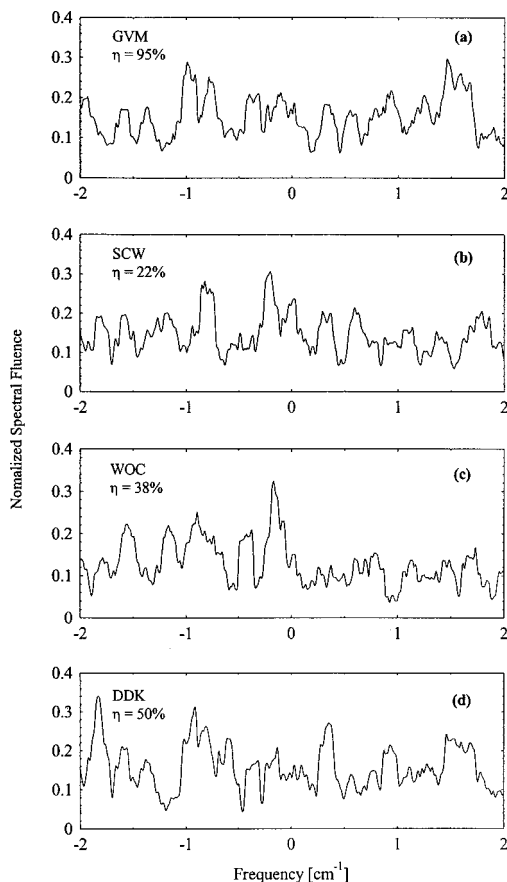


Fig. 7. Expanded view of the spectra of Fig. 6 showing that the harmonic spectra are altered significantly for strong doubling, in contrast to the weak doubling case shown in Fig. 4.

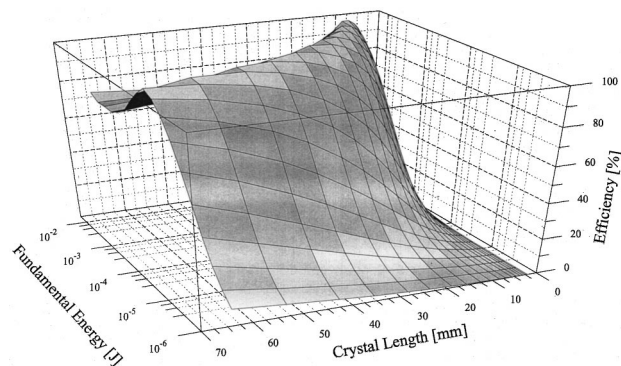


Fig. 8. Doubling efficiency versus crystal length and fundamental pulse energy for a crystal with no group-velocity walk-off (GVM).

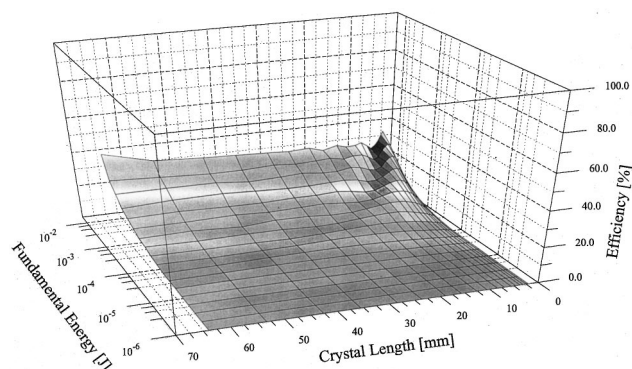


Fig. 9. Doubling efficiency versus crystal length and fundamental pulse energy for a crystal with BBO's group-velocity walk-off (SCW).

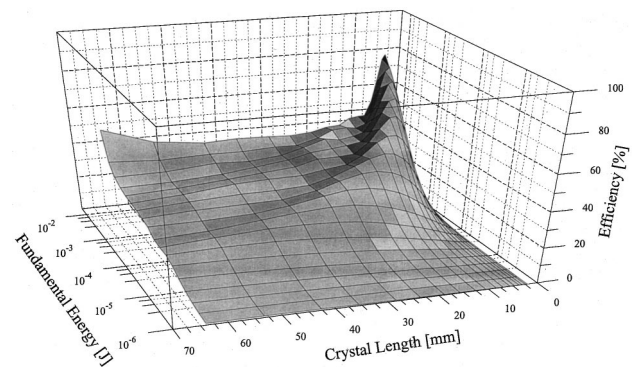


Fig. 10. Doubling efficiency versus total crystal length and fundamental pulse energy for five WOC crystals.

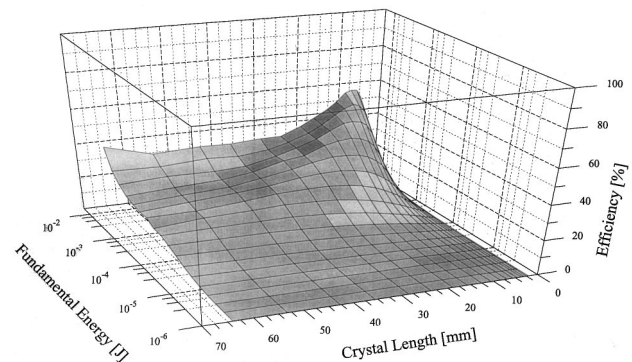


Fig. 11. Doubling efficiency versus total crystal length and fundamental pulse energy for five crystals with detunings  $\Delta k = -13.9, -6.94, 0, 6.94,$  and  $13.9 \text{ cm}^{-1}$  (DDK).

In Fig. 12 we show doubling efficiency for a fixed total crystal length of 10.54 mm as the input energy varies. Individual curves correspond to a single crystal without walk-off (GVM), a single crystal with walk-off (SCW), five crystals that are WOC, and five crystals with distributed  $\Delta k$ 's (DDK). Of the latter three, walk-off compensation is four times as efficient at low energy. The distributed  $\Delta k$  arrangement is the least efficient at low energy but increases monotonically until it is the most efficient at the highest energy. Both the WOC and the SCW cases show saturation, but the single crystal saturates at a lower energy. Bearing in mind that real beams have a transverse

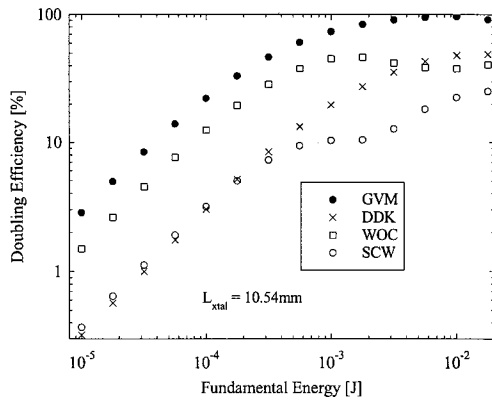


Fig. 12. Doubling efficiency versus fundamental pulse energy for a total crystal length of 10.54 mm for a single crystal with no walk-off (GVM) (filled circles), for a single crystal with walk-off (SCW) (open circles), for five WOC crystals (open squares), and for five crystals with phase-matching frequencies separated by half of the crystal acceptance bandwidth (DDK) (crosses).

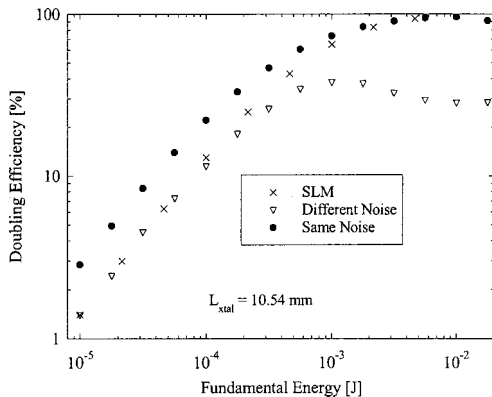


Fig. 13. Doubling efficiency versus fundamental pulse energy for a total crystal length of 10.54 mm for a single crystal with no walk-off (filled circles), for a single crystal with no walk-off and uncorrelated chaotic inputs (open triangles), and for a monochromatic input pulse (crosses).

distribution of irradiance, in most cases the WOC arrangement will give the highest efficiency among SCW, DDK, and WOC.

#### 4. CONCLUSIONS

We have modeled type I frequency doubling for broadband, 1-ns pulses of 420-nm light in BBO for two multiple-crystal configurations as well as for a single crystal with and without group-velocity differences. The primary results are contained in the surfaces of Figs. 8–11. For weakly driven doubling, analysis of the spectra and conversion efficiency for the various crystal arrangements is straightforward. We obtained the harmonic spectrum by multiplying the Fourier transform of the square of the fundamental field by an envelope function determined by the temporal walk-off and the crystal arrangement. In this regime, walk-off compensation provides both high efficiency and a broad harmonic spectrum. Distributed  $\Delta k$ 's also yield a broad spectrum but with reduced efficiency.

For strongly driven doubling, numerical modeling is essential to determine spectra and efficiencies. In this re-

gime it is possible to overdrive the crystals, resulting in less than maximum conversion efficiency. The most favorable arrangement is the matched fundamental and harmonic group velocities (GVM). This is not surprising because the acceptance bandwidth becomes much larger than the laser bandwidth when the group velocities are matched. Matching the group velocities can often be achieved with noncollinear phase matching<sup>7–10</sup> at the cost of added complexity and perhaps limited interaction lengths. With group-velocity matching the efficiency can approach 100%. The maximum efficiencies for the other arrangements are 25% for a SCW, 50% for WOC crystals, and 50% for distributed DDK. GVM and the multiple-crystal configurations, WOC and DDK, produce a larger bandwidth harmonic than a single crystal with group-velocity differences (SCW).

The type I doubling studied here is of limited generality in that the two input waves are identical and do not walk off from one another. If instead the input is two uncorrelated chaotic waves, the efficiency will be limited by a photon imbalance between the two input beams, even in the absence of temporal walk-off. The locally weaker input wave will be depleted completely some distance into the crystal. Past this point it will be regenerated with a reversed phase. The stronger wave will also grow whereas the sum-frequency wave will be depleted. In Fig. 13 we show mixing efficiency versus input energy for identical fundamental waves (filled circles), for uncorrelated chaotic input waves (open triangles), and for monochromatic pulses (crosses). Walk-off in each case is zero, but all other parameters are identical to our example case above. The uncorrelated efficiency is initially half of that of the correlated case and identical to the monochromatic case, but saturates at an efficiency of only approximately 30% because of photon imbalance.

We end with a reminder that, for multiple crystals, the relative signs of the effective nonlinear coefficient are important,<sup>17</sup> as are the intercrystal phase shifts. Finally we recommend the SNLO function PW-mix-BB (plane wave–mix–broadband)<sup>10</sup> as a fast and simple approach to the simulation of broadband mixing in a single crystal.

#### ACKNOWLEDGMENTS

This research was supported by the U.S. Department of Energy under contract DE-AC04-94AL85000. Sandia is a multiprogram laboratory operated by Sandia Corporation, a Lockheed Martin Company, for the U.S. Department of Energy.

#### REFERENCES AND NOTES

1. M. Brown, "Increased spectral bandwidths in nonlinear conversion processes by use of multicrystal designs," *Opt. Lett.* **23**, 1591–1593 (1998).
2. A. Babushkin, R. S. Craxton, S. Oskoui, M. J. Guardalben, R. L. Keck, and W. Seka, "Demonstration of the dual-tripler scheme for increased-bandwidth third-harmonic generation," *Opt. Lett.* **23**, 927–929 (1998).
3. D. Eimerl, J. M. Auerbach, C. E. Barker, D. Milam, and P. W. Milonni, "Multicrystal designs for efficient third-harmonic generation," *Opt. Lett.* **22**, 1208–1210 (1997).
4. P. W. Milonni, J. M. Auerbach, and D. Eimerl, "Frequency-

- conversion modeling with spatially and temporally varying beams," in *Solid State Lasers for Application to Inertial Confinement Fusion (ICF)*, W. F. Krupke, ed., Proc. SPIE **2633**, 230–241 (1997).
5. A. V. Smith, D. J. Armstrong, and W. J. Alford, "Increased acceptance bandwidths in optical frequency conversion by use of multiple walk-off-compensating nonlinear crystals," *J. Opt. Soc. Am. B* **15**, 122–141 (1998).
  6. R. J. Gehr, M. W. Kimmel, and A. V. Smith, "Simultaneous spatial and temporal walk-off compensation in frequency-doubling femtosecond pulses in  $\beta$ -BaB<sub>2</sub>O<sub>4</sub>," *Opt. Lett.* **23**, 1298–1300 (1998).
  7. B. A. Richman, S. E. Bisson, R. Trebino, E. Sidick, and A. Jacobson, "Efficient broadband second-harmonic generation by dispersive achromatic nonlinear conversion using only prisms," *Opt. Lett.* **23**, 497–499 (1998).
  8. R. Danielius, A. Piskarskas, P. Di Trapani, A. Andreoni, C. Solcia, and P. Foggi, "A collinearly phase-matched parametric generator/amplifier of visible femtosecond pulses," *IEEE J. Quantum Electron.* **34**, 459–463 (1998).
  9. T. Wilhelm, J. Piel, and E. Riedle, "Sub-20-fs pulses tunable across the visible from a blue-pumped single-pass noncollinear parametric converter," *Opt. Lett.* **22**, 1494–1496 (1997).
  10. The function GVD is within SNLO. The SNLO nonlinear optics code is available from A. V. Smith at the following web site: <http://www.sandia.gov/imrl/X1118/xxxtal.htm>.
  11. A. V. Smith and R. J. Gehr, "Numerical models of broad-bandwidth nanosecond optical parametric oscillators," *J. Opt. Soc. Am. B* **16**, 609–619 (1999).
  12. W. J. Alford, R. J. Gehr, R. L. Schmitt, A. V. Smith, and G. Arisholm, "Beam tilt and angular dispersion in broad-bandwidth, nanosecond optical parametric oscillators," *J. Opt. Soc. Am. B* **16**, 1525–1532 (1999).
  13. S. E. Kurtz, "Measurement of nonlinear optical susceptibilities," in *Quantum Electronics*, H. Rabin and C. L. Tang, eds. (Academic, New York, 1975), Vol. 1, Part, A, pp. 209–281.
  14. See Figs. 15 and 16 of Ref. 5.
  15. M. A. Norton, D. Eimerl, C. A. Ebberts, S. P. Velsko, and C. S. Petty, "KD\*P frequency doubler for high average power applications," in *Solid State Lasers*, G. Duke, ed., Proc. SPIE **1223**, 75–83 (1990).
  16. R. C. Eckardt and J. Reintjes, "Phase matching limitations of high efficiency second harmonic generation," *IEEE J. Quantum Electron.* **QE-20**, 1178–1187 (1984).
  17. D. J. Armstrong, W. J. Alford, T. D. Raymond, A. V. Smith, and M. S. Bowers, "Parametric amplification and oscillation with walkoff-compensating crystals," *J. Opt. Soc. Am. B* **14**, 460–474 (1997).